The EMBO Journal (2013) 32, 1977–1989
www.embojournal.org

SOURCE DATA | TRANSPARENT PROCESS

THE EMBO JOURNAL

Wnt/β-catenin signalling induces MLL to create epigenetic changes in salivary gland tumours

Peter Wend[1,7], Liang Fang[1], Qionghua Zhu[1], Jörg H Schipper[2], Christoph Loddenkemper[3], Frauke Kosel[1], Volker Brinkmann[4], Klaus Eckert[1], Simone Hindersin[2], Jane D Holland[1], Stephan Lehr[5], Michael Kahn[6], Ulrike Ziebold[1,8] and Walter Birchmeier[1,8,*]

[1]Max-Delbrueck Center for Molecular Medicine, Berlin, Germany, [2]Department of Otorhinolaryngology, University Hospital Düsseldorf, Düsseldorf, Germany, [3]Institute of Pathology, Charité-UKBF, Berlin, Germany, [4]Max Planck Institute for Infection Biology, Berlin, Germany, [5]Baxter Innovations GmbH, Vienna, Austria and [6]Eli and Edythe Broad Center for Regenerative Medicine and Stem Cell Research, University of Southern California, Los Angeles, CA, USA

We show that activation of Wnt/β-catenin and attenuation of Bmp signals, by combined gain- and loss-of-function mutations of β-catenin and Bmpr1a, respectively, results in rapidly growing, aggressive squamous cell carcinomas (SCC) in the salivary glands of mice. Tumours contain transplantable and hyperproliferative tumour propagating cells, which can be enriched by fluorescence activated cell sorting (FACS). Single mutations stimulate stem cells, but tumours are not formed. We show that β-catenin, CBP and Mll promote self-renewal and H3K4 tri-methylation in tumour propagating cells. Blocking β-catenin–CBP interaction with the small molecule ICG-001 and small-interfering RNAs against β-catenin, CBP or Mll abrogate hyperproliferation and H3K4 tri-methylation, and induce differentiation of cultured tumour propagating cells into acini-like structures. ICG-001 decreases H3K4me3 at promoters of stem cell-associated genes *in vitro* and reduces tumour growth *in vivo*. Remarkably, high Wnt/β-catenin and low Bmp signalling also characterize human salivary gland SCC and head and neck SCC in general. Our work defines mechanisms by which β-catenin signals remodel chromatin and control induction and maintenance of tumour propagating cells. Further, it supports new strategies for the therapy of solid tumours.

The EMBO Journal (2013) **32,** 1977–1989. doi:10.1038/emboj.2013.127; Published online 4 June 2013
Subject Categories: signal transduction; chromatin & transcription; molecular biology of disease
Keywords: cancer; epigenetics; therapy; tumour propagating cells/cancer stem cells; Wnt/beta-catenin

*Corresponding author. Max-Delbrueck-Center for Molecular Medicine, Robert-Rössle-Strasse 10, Berlin 13125, Germany. Tel.: +49 30 9406 3800; Fax: +49 30 9406 2656; E-mail: wbirch@mdc-berlin.de
[7]Present address: David Geffen School of Medicine and Jonsson Comprehensive Cancer Center, University of California, Los Angeles, CA 90095, USA.
[8]These senior authors contributed equally to this work.

Received: 25 October 2012; accepted: 7 May 2013; published online: 4 June 2013

Introduction

Tumour propagating cells or cancer stem cells exhibit stem cell- or progenitor-like properties, that is, they are able to either self-renew or differentiate into multiple cell types (Sneddon and Werb, 2007; Ben-Porath *et al*, 2008; Barker *et al*, 2009). Understanding molecular mechanisms that regulate tumour propagating cells may help to develop rational therapies. Canonical Wnt signalling maintains many embryonic and adult stem cell types; this signalling system also contributes to the generation of tumour propagating cells (Clevers, 2006; Grigoryan *et al*, 2008; Malanchi *et al*, 2008; Wend *et al*, 2010). Conversely, Bmp signalling inhibits the tumorigenic potential of cancer stem cells of the brain (Piccirillo *et al*, 2006).

Wnt/β-catenin signals control transcription and gene expression through Wnt response elements (WRE) that are recognized by the β-catenin–LEF/TCF complex, and modulate chromatin structure (Behrens *et al*, 1996; Molenaar *et al*, 1996; Mosimann *et al*, 2009). Hallmarks of chromatin states are modifications on the tails of core histones: tri-methylation of lysines 4, 9 and 27 of histone H3 (H3K4me3, H3K9me3 and H3K27me3) is associated with active chromatin, heterochromatin and repressed chromatin, respectively (Goldberg *et al*, 2007; Albert and Peters, 2009). Various chromatin modifiers are recruited to the C-terminus of β-catenin (Mosimann *et al*, 2009). In *Drosophila*, β-catenin recruits CBP; the histone acetyltransferase (HAT) activity of CBP acetylates chromatin over wide regions surrounding particular WRE (Parker *et al*, 2008). β-Catenin also interacts with histone methyltransferase MLL that promotes H3K4 tri-methylation (Sierra *et al*, 2006).

The developing salivary glands of human and mice are complex secretory organs, which in mice begin to develop from a simple epithelial bud around embryonic day (E)11.5–12.5 (Tucker, 2007). The mature glands include luminal ductal, acinar and intercalated duct cells that intermingle with stem cells, which express CD24 and CD29 surface markers (Hisatomi *et al*, 2004; Nanduri *et al*, 2011). Salivary gland stem cells contribute to maintenance and regeneration of the adult salivary glands in rodents and can amend the function of irradiated salivary glands after stem cell transplantation (Man *et al*, 2001; Lombaert *et al*, 2008; Nanduri *et al*, 2011). Regeneration of mouse salivary glands was recently found to depend on Wnt/β-catenin signals (Hai *et al*, 2010).

Head and neck carcinomas in humans amount to 6% of all cancers (Stewart and Kleihues, 2003), the majority being squamous cell carcinomas (SCC). SCC may originate from epithelial stem or progenitor cells of the epidermis or the mucous membranes. Subpopulations of cells from human head and neck SCC with tumour propagating cell properties have recently been isolated, based on the markers CD44 and ALDH (Prince *et al*, 2007; Clay *et al*, 2010). Salivary gland carcinomas constitute only a fraction of head and neck

cancers, and 8% are SCC, which often arise in the glandula parotis (Speight and Barrett, 2002). Salivary gland SCC are aggressive, produce early lymphogenic metastases, and have a poor prognosis (Ying *et al*, 2006).

This study demonstrates that high-grade salivary gland SCC and head and neck SCC in general rely on high Wnt/β-catenin and low Bmp signalling for proliferation and self-renewal. In SCC, tumour propagating cells depend on the β-catenin–CBP complex but also MLL for the generation of an open chromatin state and the induction of a stem cell-associated gene signature. Knowing that specific Wnt/β-catenin inhibition can revert the chromatin state and lead to differentiation and tumour remission *in vivo* provides a step to safely eradicate tumour propagating cells.

Results

Head and neck SCC in humans and mice display high Wnt/β-catenin and attenuated Bmp signals

In all, 18 human salivary gland SCC and 29 other head and neck cancer of the SCC subtype were examined for Wnt/β-catenin and Bmp signalling activity (Supplementary Table 1). The majority of tumours exhibited nuclear β-catenin, a hallmark of high canonical Wnt signals (Behrens *et al*, 1996; Grigoryan *et al*, 2008), and were negative for nuclear pSmad 1/5/8 (Whitman, 1998), indicating that Bmp signals were low (Figure 1A). Nuclear β-catenin accumulated at tumour fronts (arrows on the left) (Fodde and Brabletz, 2007), whereas nuclear pSmad persisted in differentiated central areas (arrow in inset on the right). In all, 75% of grade 3 salivary gland SCC (SG-SCC), the most aggressive cancers, displayed nuclear β-catenin and were negative for pSmad, whereas only 25% of grade 2 tumours displayed these characteristics (Figure 1B, upper left; tumour grading criteria were as defined in Barnes *et al*, 2005). Similarly, two thirds of grade 3 head and neck SCC (HN-SCC) showed high nuclear β-catenin and low pSmad staining (Figure 1B, upper right). Cells with nuclear β-catenin at the tumour fronts also co-expressed cytokeratin (CK)10, which is a marker for squamous cell carcinoma (Chu and Weiss, 2002) (Supplementary Figure 1A). A subset of nuclear β-catenin-positive cells from human SG-SCC and HN-SCC co-expressed the marker CD24 (Figure 1A* and C, left; quantifications are shown in B, lower panels, percentages refer to all tumour cells) (Visvader and Lindeman, 2008; Monroe *et al*, 2011) and the marker CD44, which is specific for tumour propagating cells in HN-SCC (Figure 1C, right; quantifications for grade 2 and grade 3 tumours are depicted in yellow letters below insets) (Prince *et al*, 2007; Visvader and Lindeman, 2008).

To gain mechanistic insights into the relevance of β-catenin and BMP signals in tumour formation of salivary gland SCC, we created a mouse model. Combined β-catenin gain-of-function (β-cat^{GOF}) and Bmp receptor 1a loss-of-function (Bmpr1a^{LOF}) mutations were introduced by Cre recombinase driven by the *Keratin 14* gene, referred to as double mutants (Harada *et al*, 1999; Huelsken *et al*, 2001; Mishina *et al*, 2002) (see breeding scheme in Supplementary Figure 1F). K14-Cre activity was confirmed by using a LacZ indicator mouse line; recombination occurred in ductal cells of the salivary glands (Supplementary Figure 1B–E and G). Aggressive tumours appeared rapidly in the salivary glands of the double mutants (Figure 1D, a schematic view of the normal mouse salivary glands is provided in http://www.informatics.jax.org/cookbook/figures/figure45.shtml). Kaplan–Meier plots show that double mutants succumbed to tumours rapidly, dying between postnatal day (P)75 and P90 (Figure 1E). After full necroscopy, a pathologist (CL) determined that these tumours exclusively arose from the submandibular salivary glands. The tumours were classified as SG-SCC by histopathological criteria, contained keratin pearls and expressed high levels of CK10 (Supplementary Figure 2A, right, see also inset) (Chu and Weiss, 2002; Barnes *et al*, 2005). Moreover, consistent with the human tumours, mouse SG-SCC also showed high Wnt/β-catenin and low Bmp signals, as determined by staining for β-catenin, the Wnt target gene Axin2 and pSmad1/5/8 (Supplementary Figure 2B). Neither single β-cat^{GOF} nor Bmpr1a^{LOF} mutant mice did develop tumours (Figure 1E; Supplementary Figure 2A, middle panels). Gene expression profiling and gene set enrichment analysis (GSEA) at P1 and P90 revealed that in double-mutant salivary glands, genes associated with proliferation as *c-myc* and differentiation/apoptosis as *Loricrin* or *Fas* were upregulated and downregulated, respectively, when compared to β-cat^{GOF} tissues (Supplementary Figure 2C; Supplementary Tables 2 and 3, see also below). Other K14-expressing tissues of double mutants did not develop tumours; while epithelia of the esophagus and forestomach showed no significant histological changes, we observed excessive supernumerary hair follicles in the skin, when compared to wild-type mice (Supplementary Figure 2D). Taken together, the fast accumulation of salivary gland SCC in the double-mutant mice was the net result of strong proliferation and reduced differentiation and apoptosis.

Wnt/β-catenin and Bmp signals control tumour propagating cells in salivary gland SCC

In order to characterize cells that are specific and essential for tumour formation in double-mutant salivary glands, we isolated CD24$^+$CD29$^+$ cells by fluorescence activated cell sorting (FACS) from glands of the different genotypes; these surface markers have been previously used to enrich for stem cells of salivary glands (Hisatomi *et al*, 2004; Visvader and Lindeman, 2008; Nanduri *et al*, 2011). The proportion of CD24$^+$CD29$^+$ cells increased three-fold and ten-fold in single and double mutants, respectively, compared to controls (Figure 2A; Supplementary Figure 3A–C). Enrichment of CD24$^+$ cells could be confirmed by immunofluorescence analysis (Figure 2B). Isolated CD24$^+$CD29$^+$ cells were collected by cytospin and their proliferation was assessed using Ki67 antibody staining (Figure 2C). CD24$^+$CD29$^+$ cells from double-mutant salivary glands were hyperproliferative: over 80% were Ki67$^+$ (Figure 2D), compared to 13% non-sorted cells (Figure 2E). High proliferation was confirmed by FACS for Ki67, which showed that over 90% of CD24$^+$CD29$^+$ cells were highly proliferating (P1 cells in Supplementary Figure 4A and B). Another strongly proliferative CD24$^-$ subpopulation (up to 40% Ki67$^+$) was identified, but these were not epithelial cells and instead expressed stromal markers (P4 cells; Supplementary Figure 4A and B, and data not shown). The salivary gland tumours stained weakly for Sca-1 or c-kit (not shown) (Hisatomi *et al*, 2004), and the CD24$^+$CD29$^+$ subpopulation co-expressed the marker CD44 only at low

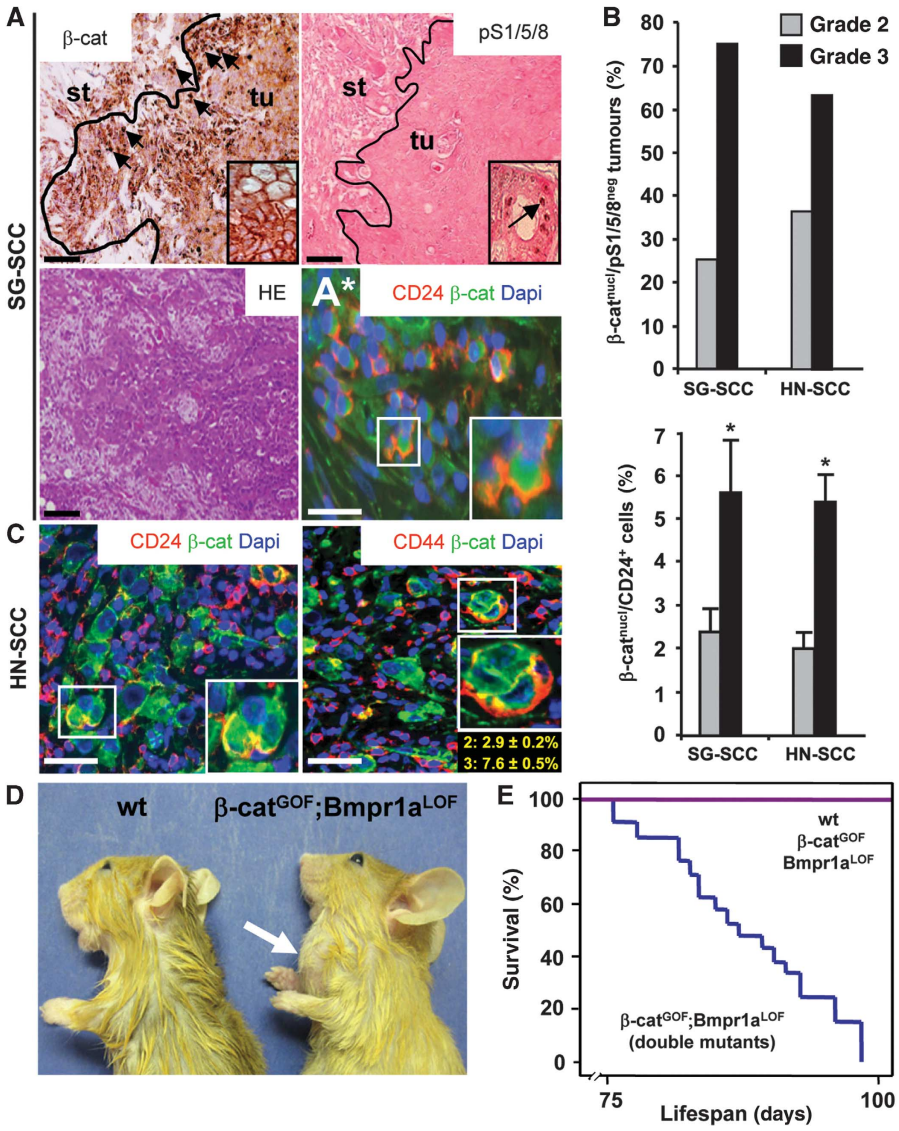

Figure 1 High Wnt/β-catenin and low Bmp signalling characterize head and neck squamous cell carcinoma of humans and mice. (**A**) Serial sections of human salivary gland SCC, as analysed by immunohistochemistry for β-catenin and pSmad1/5/8 or by H&E staining; at tumour fronts, β-catenin is located in nuclei (black arrows) and at cell junctions in differentiated, central tumour areas (inset), whereas phospho-Smad1/5/8 staining is low (inset shows nuclear pSmad1/5/8 staining in tubular cells from a differentiated, central area of the same tumour, see arrow). (A*) Immunofluorescence for CD24 (in red) and β-catenin (in green, DAPI in blue); CD24 co-localizes with nuclear β-catenin. st, stroma; tu, tumour. (**B**) Upper graphs: the specific combination of nuclear β-catenin and negative pSmad 1/5/8 was detected in 75% of aggressive, grade 3 human salivary gland SCC (SG-SCC) and in 63% of grade 3 head and neck SCC (HN-SCC). (**C**) Sections of human HN-SCC, as analysed by immunofluorescence for the stem cell markers CD24 and CD44 (in red) and β-catenin (in green, DAPI in blue). CD24 and CD44 co-localize with nuclear β-catenin in head and neck SCC (quantitation is in **B**, lower graph, and in **C**, right panel, in yellow letters for grade 2 and grade 3 tumours: the number of double-positive cells for nuclear β-catenin and CD24 was upregulated in grade 3 SG-SCC and HN-SCC; percentages refer to all tumour cells). The bars give means and standard deviations (*$P<0.05$, Student's *t*-test). *P*-values are as compared with grade 2 tumours. (**D**) Side view of control (wt) and K14Cre;β-cat^{GOF}:Bmpr1a^{LOF} double-mutant mice at P90 (arrow marks a salivary gland tumour). (**E**) Kaplan–Meier survival plot of double-mutant tumour mice, compared to control and single mutant mice without tumours (each group $n=21$). Bar, 200 μm in (**A**) and 50 μm in (**A***, **C**).

levels (Supplementary Figure 3D and E). To examine the tumour-propagating potential, CD24$^+$CD29$^+$ cells of double mutants and various control cell populations were injected into the back skin of NOD/SCID mice (Figure 2F; Visvader and Lindeman, 2008). As few as 500 CD24$^+$CD29$^+$ cells from double-mutant glands produced fast-growing tumours, while cells that expressed only high CD24 or CD29 did not produce fast-growing tumours (Figure 2F and G; Supplementary Figure 4C). Unsorted cells from double-mutant glands were only moderately tumorigenic, at 10^5 but not at 10^4 injected cells (Figure 2F). Tumours arising from transplanted cells co-expressed the SCC markers CK10 and CK14, and contained differentiated and undifferentiated areas (Supplementary Figure 4D and E). Transplanted tumours maintained stable subpopulations of CD24$^+$CD29$^+$ cells in serial transplantations that retained high tumour propagating potential (Supplementary Figure 4F and G). From these results, we conclude that CD24$^+$CD29$^+$ cells from double-mutant salivary gland SCC are highly enriched for tumour propagating cells.

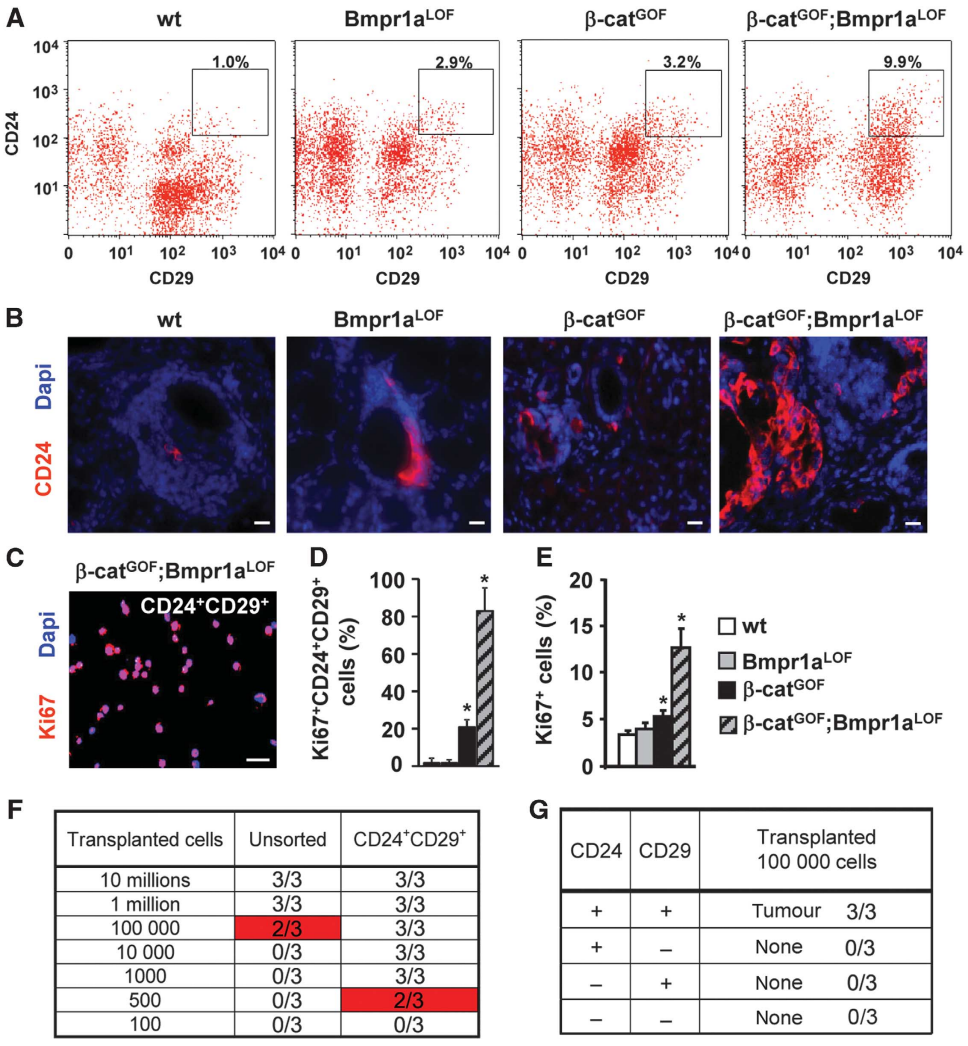

F

Transplanted cells	Unsorted	$CD24^+CD29^+$
10 millions	3/3	3/3
1 million	3/3	3/3
100 000	2/3	3/3
10 000	0/3	3/3
1000	0/3	3/3
500	0/3	2/3
100	0/3	0/3

G

CD24	CD29	Transplanted 100 000 cells	
+	+	Tumour	3/3
+	–	None	0/3
–	+	None	0/3
–	–	None	0/3

Figure 2 Wnt/β-catenin and Bmp signalling control tumour propagating cells in salivary glands of mice. (**A**) FACS analysis of control (wt) and mutant salivary gland cells. High $CD24^+CD29^+$ expressing cells are marked by squares (insets), and quantification is shown above the squares (details on isotype control staining are shown in Supplementary Figure 3). (**B**) Sections of control and mutant salivary glands stained by immunofluorescence for CD24 (in red, DAPI in blue). (**C**, **D**) Identification of proliferating cells within the $CD24^+CD29^+$ salivary gland cell populations of all genotypes by immunofluorescence of cytospins for Ki67 (in red, DAPI in blue). Staining of double-mutant cells is shown in (**C**), quantification for all genotypes is shown in (**D**) ($n=3$). The bars give means and standard deviations (*$P<0.05$, Student's *t*-test). *P*-values are as compared with wild-type cells. Bar, 25 μm. (**E**) Quantification of proliferation in salivary gland cells of control and mutant mice, as determined by immunofluorescence for Ki67 ($n=3$). The bars give means and standard deviations (*$P<0.05$, Student's *t*-test). *P*-values are as compared with wild-type cells. (**F**) Tumour outgrowths produced from subcutaneous injections of different cell numbers of unsorted or sorted $CD24^+CD29^+$ cells from β-cat^{GOF};$Bmpr1a^{LOF}$ double-mutant glands into the back skin of NOD/SCID mice (each group $n=3$, details on serial transplantations are provided in Supplementary Figure 4F and G). (**G**) Tumour formation capacity of other sorted subpopulations of cells of β-cat^{GOF};$Bmpr1a^{LOF}$ double-mutant glands (each group $n=3$). Single $CD24^+$ or $CD29^+$ or $CD24^-/CD29^-$ cells from double-mutants did not produce tumours.

Salivary gland tumour propagating cells are characterized by a stem cell-associated gene signature and specific chromatin marks

To elucidate mechanisms that potentiate the self-renewal of tumour propagating cells, we examined stem cell-associated genes that were co-expressed with activated Wnt/β-catenin (Ben-Porath *et al*, 2008; Wend *et al*, 2010). Remarkably, tumour propagating cells of double mutants expressed embryonic-type $SSEA1^+$ (Figure 3A) (Read *et al*, 2009). The SSEA1 expression specifically characterized cells with high Wnt/β-catenin signals since >90% of the $CD24^+CD29^+SSEA1^+$ triple-sorted cells exhibited nuclear β-catenin, which was not found in other subpopulations (Figure 3B, and data not shown). $CD24^+CD29^+$ cells were also characterized by low pSmad1/5/8 intensity, as compared to unsorted tumour cells (Supplementary Figure 5A and B). Gene expression profiling of $CD24^+CD29^+$ cells revealed that a number of genes associated with the pluripotent state were highly expressed (Supplementary Figure 5C and D; Supplementary Table 4). Among those were Nr5a2, which can replace Oct4 in reprogramming of iPS cells (Heng *et al*, 2010), the ES-cell associated Snf2-like helicase Hells (Xi *et al*, 2009), the stem cell marker Dppa5 (Ware *et al*, 2009) and the stem cell-associated chromatin modifiers Ash2, Mll (Dou *et al*, 2005) and Rnf2 (De Napoles *et al*, 2004). A GSEA confirmed that genes important for pluripotent stages in organism development were enriched in double-mutant tumour propagating cells (Supplementary Table 3).

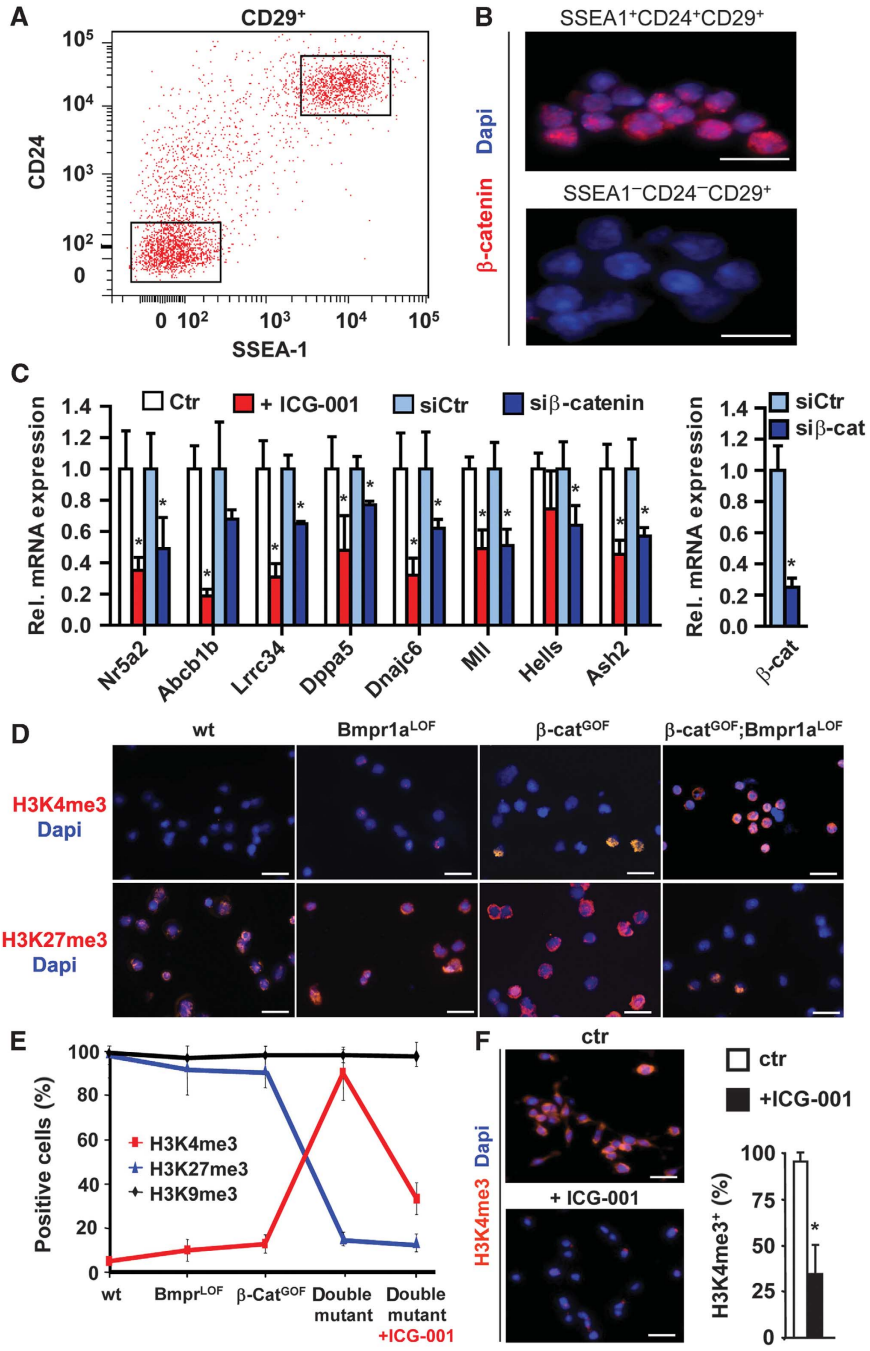

Figure 3 Salivary gland tumour propagating cells of double-mutant mice are characterized by stem cell-associated gene expression and specific chromatin marks. (**A**) FAC-sorted CD29$^+$ salivary gland tumour propagating cells were further sorted for CD24 and SSEA-1 expression (high or low expressing cells are gated, insets). (**B**) Immunofluorescence of triple-sorted SSEA-1$^+$ and SSEA-1$^-$ cells for nuclear β-catenin (in red, DAPI in blue). (**C**) qRT–PCR of highly expressed genes in sorted CD24$^+$CD29$^+$ tumour propagating cells at P75–80, which were identified by Affymetrix microarray analysis (details shown in Supplementary Figure 5B and C and Supplementary Table S4), and downregulation following treatment with the Wnt/β-catenin inhibitor ICG-001 or β-catenin siRNA ($n=4$). (**D**) Analysis of histone tri-methylation patterns by immunofluorescence for H3K4me3 and H3K27me3 of cytospins of CD24$^+$CD29$^+$ salivary gland cells (in red, DAPI in blue, quantification is shown in **E**). (**E**) Histone tri-methylation revealed a profound switch of chromatin marks in the double-mutant tumour propagating cells. Immunofluorescence for H3K9me3 is shown in Supplementary Figure 5D. (**F**) H3K4me3 (in red, DAPI in blue) is suppressed in tumour propagating cells upon treatment with ICG-001 at 25 μM (for quantification of H3K9me3 and H3K27me3 after ICG-001, see (**E**). The vertical bars give means and standard deviations (*$P<0.05$, Student's *t*-test). *P*-values are as compared with controls (**C**, **F**). Bars of magnifications in (**B**, **D**, **F**); 25 μm.

Treatment for 24 h with ICG-001, an inhibitor of canonical Wnt signalling that blocks β-catenin–CBP interaction (Emami *et al*, 2004), and small-interfering RNA (siRNA)-mediated downregulation of β-catenin significantly suppressed these genes (Figure 3C).

Previous research has shown that the maintenance of pluripotency is linked to the epigenetic state of cells (Surani *et al*, 2007; Albert and Peters, 2009; Wend *et al*, 2010). Remarkably, sorted CD24$^+$CD29$^+$ tumour propagating cells from double-mutant salivary glands showed a marked

increase in H3K4me3, as assessed by immunohistological analysis of cytospins, which was low in $CD24^+CD29^+$ cells from wild-type and single mutant tissue (Figure 3D, quantified in E). H3K4me3 generally characterizes transcriptionally active promoters, but high enrichment is also indicative of stem cell promoters (Albert and Peters, 2009; Wend *et al*, 2010; Gaspar-Maia *et al*, 2011). In contrast, $CD24^+CD29^+$ cells from double mutants showed a low level of H3K27me3, compared to $CD24^+CD29^+$ cells from wild-type and single mutants (Figure 3D and E), whereas the H3K9me3 levels were similar in all genotypes (Figure 3E; Supplementary Figure 5E). These epigenetic marks in $CD24^+CD29^+$ cells from double mutants require high Wnt/β-catenin: after 24 h of ICG-001 treatment, the numbers of H3K4me3-positive cells declined by $>60\%$ (Figure 3F). Similar changes in H3K4me3 and H3K27me3, but not in H3K9me3, were also observed by western blot analysis of extracts from salivary glands of control and mutant mice, and in tumours that arose from transplanted cells (Supplementary Figure 5F). Thus, the specific alterations in chromatin-associated histone marks suggest that the overall epigenetic makeup has changed in the tumour propagating cells of the salivary glands. Further, tumour propagating cells are distinguished by the expression of a gene signature that is associated with pluripotency.

To examine whether activated canonical Wnt signalling affects human salivary SCC in a similar manner, we assessed H3K4me3 and nuclear β-catenin levels in human tumours, which could be detected preferentially at the invasive tumour fronts (Supplementary Figure 5G). We also investigated several tumour cell lines of human head and neck SCC. Endogenous Wnt signalling activity in these cells was variable, as assessed by the expression of the Wnt/β-catenin target gene Axin2 (Lustig *et al*, 2002; Grigoryan *et al*, 2008). Typically, cell lines with high and low Wnt activity (e.g., HN-SCCUM-03T and HN-SCCUM-02T) displayed opposite, that is, low and high pSmad1/5/8 levels, respectively (Supplementary Figure 6A). HNSCCUM-03T cells with high Wnt activity were treated with ICG-001, which downregulated the expression of stem cell-associated signature genes *NR5A2*, *ABCB1B*, *LRRC34 DNAJC6* and of the genes encoding chromatin modifiers *HELLS*, *MLL* and *ASH2* (Supplementary Figure 6B). Conversely, CHIR 99021, a Wnt activator (Ring *et al*, 2003), upregulated the expression of these genes in HNSCCUM-02T cells that display low endogenous Wnt signals (Supplementary Figure 6B). Interestingly, a large number of HNSCCUM-03T cells with high Wnt co-expressed CD44, a stem cell marker of human SCC tumours, as well as CD24, whereas HNSCCUM-02T cells with low Wnt only co-expressed CD24 and CD44 after Wnt activation, that is, 48 h exposure to CHIR 99021 (Supplementary Figure 6A and C) (Monroe *et al*, 2011). Collectively, mouse salivary gland and human head and neck SCC cells depend on high canonical Wnt signals to create a permissive epigenetic environment that allows the expression of a stem cell-associated gene signature. This includes the human-specific stem cell marker CD44 (Gires, 2011).

ICG-001 treatment leads to tumour remission and reprograms salispheres to form differentiated acini-like structures

$CD24^+CD29^+$ tumour propagating cells from the tumours of double-mutant salivary glands were cultured. Remarkably, the canonical Wnt inhibitor ICG-001 strongly blocked proliferation of the $CD24^+CD29^+$ cells (Figure 4A). We then performed a therapy experiment in NOD/SCID mice, which were transplanted with $CD24^+CD29^+$ tumour propagating cells that were forming tumours (see Figure 2F): ICG-001 significantly reduced the size of the growing tumours (Figure 4B).

Stem cells from organs and tumours can often be expanded as non-adherent, sphere-like aggregates, which reflects their self-renewal capacity (Lombaert *et al*, 2008; Visvader and Lindeman, 2008; Monroe *et al*, 2011). Whereas $CD24^+CD29^+$ salivary gland cells from wild-type or single mutant mice did not grow as spheres, $CD24^+CD29^+$ cells from double mutants could be propagated as salispheres in the presence of hepatocyte growth factor, HGF (Figure 4C, left panel) (Brinkmann *et al*, 1995). In such salispheres, cells formed loose, net-like aggregates, that is, displayed undifferentiated structures (Figure 4D, left, see also below). Remarkably, in the presence of ICG-001, salispheres formed instead glandular structures that resemble salivary gland acini (Figure 4C, second panel, Figure 4D, right, the quantification of differentiation is in E). Light and electron microscopy demonstrated the formation of lumen, secretory granules and tight junctions in the acini-like structures but not in the undifferentiated salispheres (Supplementary Figure 6E and F, and data not shown). ICG-001 treatment also upregulated the expression of the gene encoding Amylase 1, an enzyme of differentiated salivary glands (Supplementary Figure 6G). Thus, $CD24^+CD29^+$ tumour propagating cells from salivary gland tumours of double-mutant mice exhibit unrestricted self-renewal in salisphere culture that depends on canonical Wnt signalling. We next analysed the effect of the HDAC inhibitor valproic acid (VPA) and the DNA methylation inhibitor 5-azacytidine (Aza) (Ware *et al*, 2009) on ICG-001-elicited responses in salispheres. Inhibition of proliferation by ICG-001 was not seen in the presence of VPA or Aza, but differentiation was blocked (Figure 4C, right panels, quantitation in Figure 4E; Supplementary Figure 6H). Furthermore, ICG-001 treatment of human HNSCCUM-03T cells with high endogenous Wnt strongly reduced their ability to form spheres (Supplementary Figure 6D). ICG-001 has been shown to inhibit the growth of Wnt/β-catenin-dependent human tumour cells (Emami *et al*, 2004; Wend *et al*, 2013). Conversely, CHIR 99021 enhanced the capacity of HNSCCUM-02T cells with low endogenous Wnt to form spheres (Supplementary Figure 6D). Thus, unrestricted self-renewal of tumour propagating cells of mouse salivary glands and of human SCC tumour cell lines in sphere culture depends on continuous Wnt signalling and on the maintenance of their specific epigenetic state.

Wnt/β-catenin signals exploit MLL-dependent H3K4 histone methylation activity to establish and maintain salivary gland tumour propagating cells

To learn about the significance of Wnt/β-catenin-dependent epigenetic regulation, we examined whether blocking β-catenin–CBP by ICG-001 leads to changes of histone modifications at gene promoters of stem cell-associated genes. Chromatin immunoprecipitation (ChIP) using anti-H3K4me3 antibodies was performed with $CD24^+CD29^+$ cells from mouse salivary gland tumours and with human HNSCCUM-03T tumour cells that display high Wnt activity. We detected

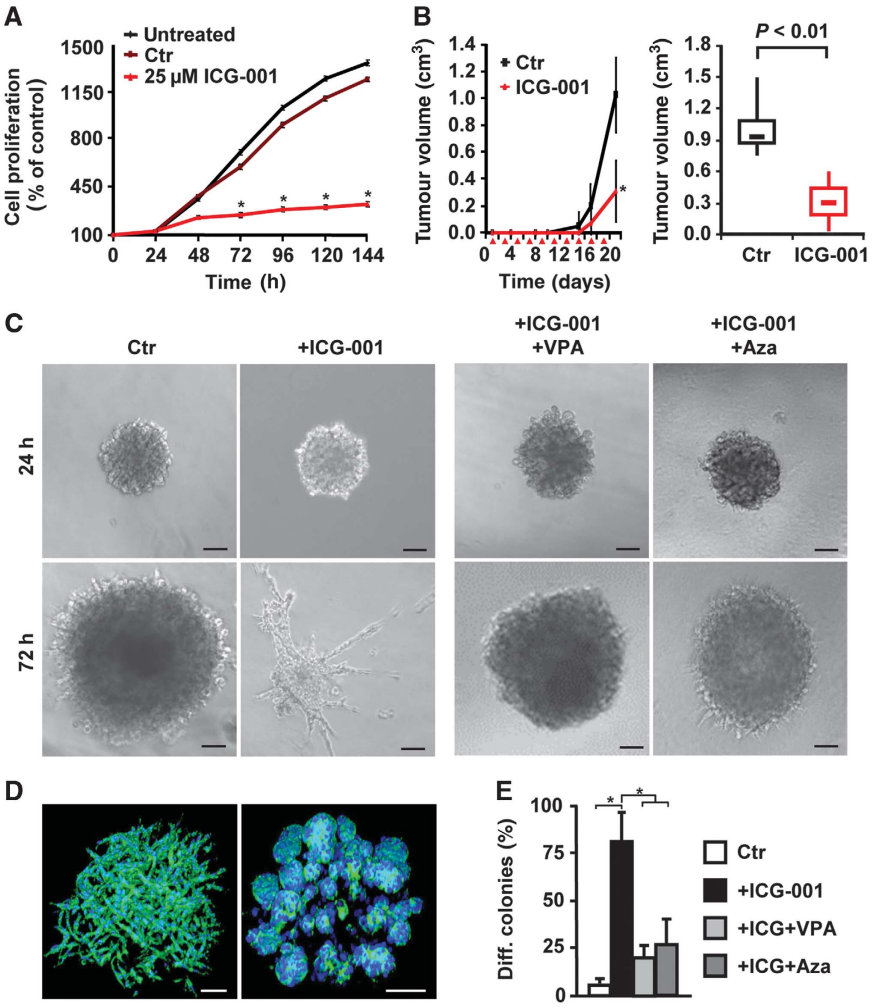

Figure 4 Salivary gland tumour propagating cells grown in non-adherent spheres (salispheres) respond to Wnt/β-catenin and HDAC and DNA methylation inhibitors. (**A**) Proliferation of tumour propagating cells and treatment with the Wnt/β-catenin inhibitor ICG-001, at 25 μM in 1% DMSO ($n=3$). (**B**) Tumour growth of transplanted tumour propagating cells in NOD/SCID mice, and inhibition after intra-peritoneal administration of ICG-001 at 200 mg/kg ($n=5$). Red triangles indicate ICG-001 administration. (**C**, left panel) Phase contrast images of undifferentiated salispheres in Matrigel cultures containing HGF, or differentiated cultures following additional treatment with ICG-001. (**C**, right panel) Reversion of differentiation of sphere cultures in the presence of additional valproic acid (VPA) or 5-azacytidine (Aza) (controls are shown in Supplementary Figure 6H). (**D**) Phalloidin staining (in green; DAPI in blue) of salispheres (left) and differentiated, gland-like structures after 72 h treatment with ICG-001 (right). (**E**) Quantifications of differentiation of spheres from (**C**) at 72 h. In (**A**, **B**, **E**), means and standard deviations are shown (*$P<0.05$, Student's *t*-test for **A**, **B**; ANOVA for **E**). *P*-values are as compared with control cells or with cells that received combined treatment. Bar in (**C**, **D**) 100 μm.

high enrichments of H3K4me3 at sequences, which are in close proximity to the promoters of *Mll*, *Hells*, *Ash2* and *c-myc* genes, but not at promoter-far sequences in the mouse and human cells (Figure 5A and B). ICG-001 significantly decreased the enrichment of H3K4me3 at promoter-proximal sequences. We also examined the sequential order of changes in H3K4me3 and in gene expression of mouse $CD24^+CD29^+$ tumour propagating cells that depend on ICG-001. H3K4me3 downregulation could be detected 12 h after ICG-001 treatment (Figure 5C). In contrast, expression changes of genes of the stem cell-associated gene signature or of the differentiation marker Amylase occur later, 24 h after ICG-001 treatment (Figure 5D). These data show that the β-catenin–CBP-interfering substance ICG-001 elicits changes in H3K4me3 at target promoters, and that the epigenetic changes precede transcriptional changes.

We next addressed the question of how abrogation of Wnt/β-catenin signals might produce the shift of epigenetic marks. Remarkably, treating $CD24^+CD29^+$ cells from double-mutant tumours with ICG-001 resulted in a significant translocation of β-catenin out of the nucleus and in cytoplasmic accumulation (Figure 6A, protein quantifications are shown above the blots). Concomitantly, Mll, a known binding partner of nuclear β-catenin with histone methyltransferase activity towards H3K4 (Sierra *et al*, 2006), disappeared from the nuclear fraction (Figure 6B). Two protein products of the stem cell signature, Hells and Nr5a2, were also downregulated (Supplementary Figure 7A). Conversely, activating Wnt/β-catenin with CHIR 99021 lead to an increase in nuclear β-catenin and nuclear Mll (Figure 6A and B). The increase in β-catenin might be due to the product of the remaining wild-type allele in the double-mutant mice (see Supplementary

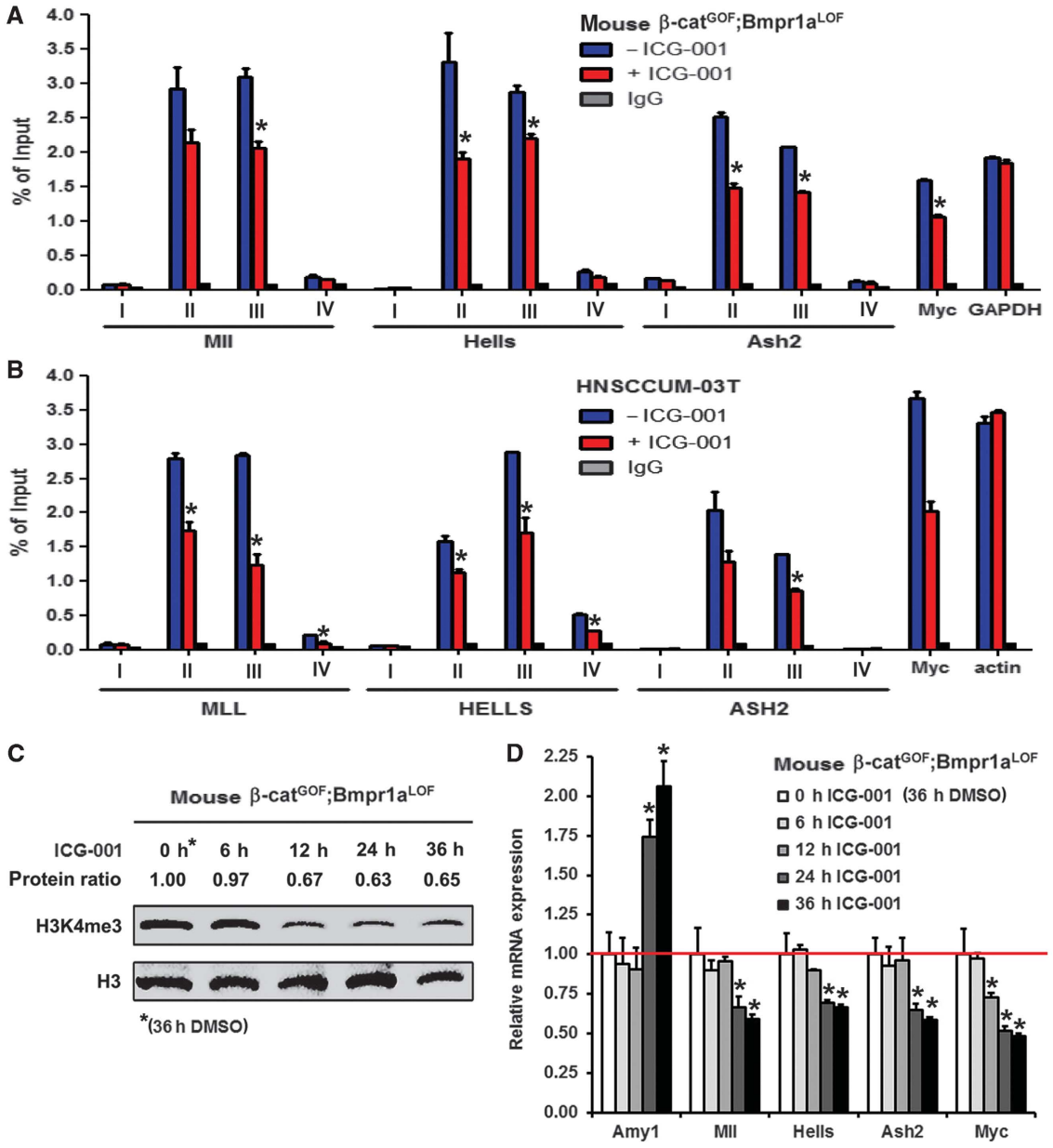

Figure 5 Chromatin immunoprecipitation (ChIP) of promoters of chromatin-modifying or Wnt/β-catenin target genes. ICG-001-induced downregulation of H3K4me3 precedes changes in gene expression in mouse tumour propagating cells and human HN-SCC tumour cells. (**A**, **B**) H3K4me3 enrichment at the promoters of *Mll*, *Hells*, *Ash2*, *Myc* and *GAPDH* or *actin* genes assessed by ChIP of mouse β-cat^{GOF};Bmpr1a^{LOF} tumour propagating cells and human head and neck tumour cells (HNSCCUM-03T) upon ICG-001 treatment ($n=3$, I + IV: amplicons from promoter-far regions; II + III: amplicons from promoter-near regions). (**C**) Western blot analysis of H3K4me3 in a time-course experiment of ICG-001-treated mouse β-cat^{GOF};Bmpr1a^{LOF} tumour propagating cells. Protein ratios depict H3K4me3 signal intensities, normalized to H3, which served as loading control. (**D**) qRT–PCR analysis of samples from the time-course experiment depicted in (**C**). Expression changes in the differentiation-associated gene *Amy1* or *Mll*, *Hells*, *Ash2* and *Myc* (genes analysed by ChIP in **A**) were quantified ($n=3$). In (**A**, **B**, **D**), means and standard deviations are shown (*$P<0.05$, Student's *t*-test). *P*-values are as compared with control cells. Source data for this figure is available on the online supplementary information page.

Figure 1F and G). Nuclear exclusion of β-catenin by inhibiting with ICG-001 could also be detected in the human high Wnt HNSCCUM-03T cells (Supplementary Figure 7B). Collectively, these data show that nuclear Mll and the expression of the stem cell-associated gene signature are dependent on the presence of high Wnt/β-catenin signals.

We next examined the potential role of Mll in the CD24$^+$CD29$^+$ cells of salivary gland tumours by performing siRNA-mediated downregulation of β-catenin, CBP and Mll. These treatments resulted in a strong reduction of the numbers of H3K4me3$^+$ and Ki67$^+$ cells (Figure 6C; Supplementary Figure 7C). Downregulation of another histone methyltransferase, Ash1, had no effect on H3K4me3 and Ki67 levels. ICG treatment and siRNA against Mll or β-catenin also profoundly reduced the proliferation of tumour propagating cells, while siRNA against Dppa5 had no effect (Figure 6D) (Kim *et al*, 2005). Mll is strongly expressed in the tumour propagating cells of salivary glands; nuclear Mll was found to be associated with the rare CD24$^+$ cells (Supplementary Figure 7E, arrows). Remarkably, knockdown of β-catenin and Mll by siRNA treatment resulted in acini formation in sphere culture, that is, forced a large fraction of

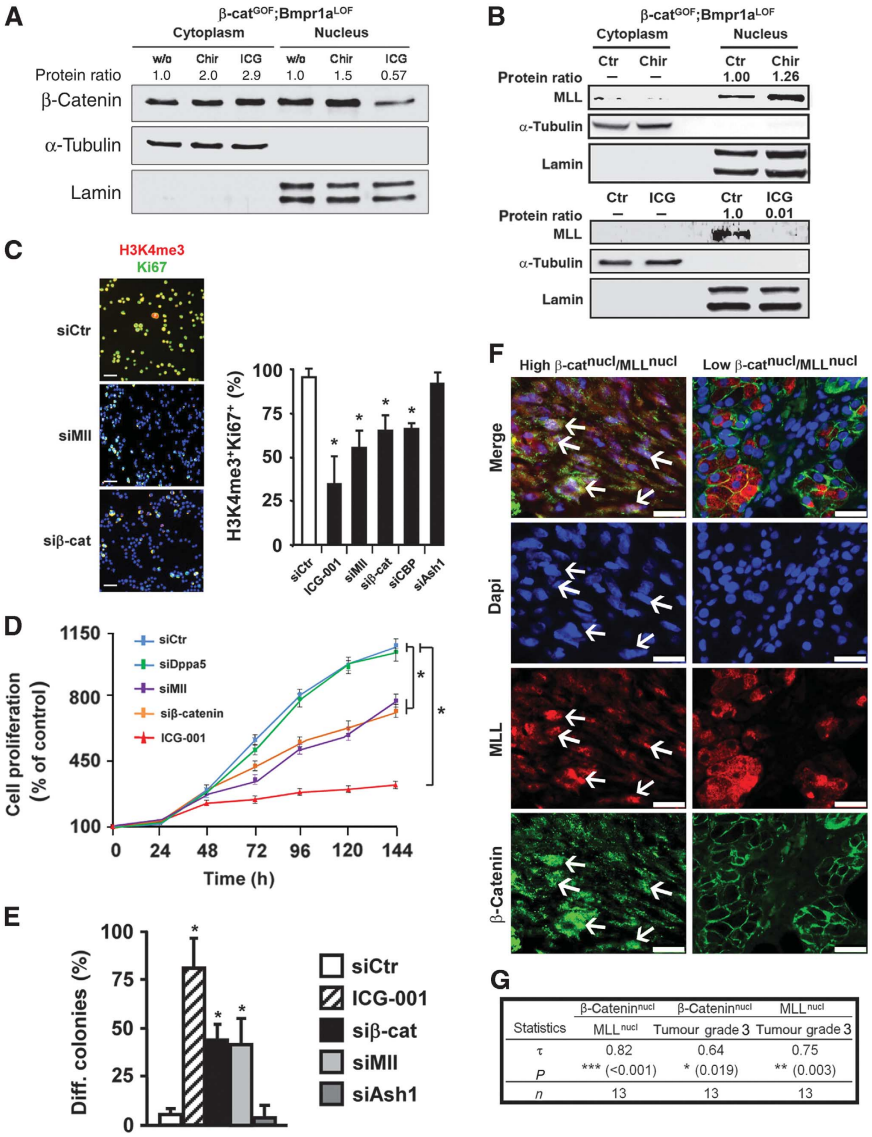

Figure 6 Wnt/β-catenin signalling exploits an MLL-dependent H3K4 activity to establish and maintain salivary gland tumour propagating cells. Co-expression of nuclear β-catenin and nuclear MLL is associated in human salivary gland SCC. (**A**) Western blot analysis of β-catenin in cytoplasmic and nuclear fractions from untreated (w/o), CHIR- or ICG-001-treated $CD24^+CD29^+$ salivary gland tumour propagating cells. (**B**) Western blot analysis of MLL in cytoplasmic and nuclear fractions of untreated (Ctr), CHIR- or ICG-001-treated tumour propagating cells. α-Tubulin and Lamin in (**A**, **B**) are the cytoplasmic or nuclear loading controls, respectively. Protein ratios in (**A**, **B**) depict β-catenin or MLL signal intensities, normalized to the corresponding loading controls. (**C**) Analysis of histone tri-methylation pattern and proliferation by immunofluorescence for H3K4me3 (in red) and Ki67 (in green, DAPI in blue), using cytospins of tumour propagating cells upon siRNA-induced knockdown of Mll, β-catenin, CBP and Ash1, or treatment with the Wnt/β-catenin inhibitor ICG-001 at 25 μM in 1% DMSO ($n=3$). Quantifications are shown on the right (siCtr, control siRNA). (**D**) Proliferation of tumour propagating cells upon siRNA-induced knockdown of Dppa5a, Mll and β-catenin, or treatment with ICG-001 ($n=3$). (**E**) Quantifications of differentiation of tumour propagating cells in 3D-Matrigel cultures upon siRNA-induced knockdown of β-catenin, Mll and Ash1, or treatment with ICG-001 ($n=4$). (**F**) Immunofluorescence analysis for β-catenin (green) and MLL (red, DAPI in blue) of human salivary gland SCC ($n=13$). Two representative tumours are shown to distinguish high $\beta\text{-catenin}^{nucl}/MLL^{nucl}$ from low $\beta\text{-catenin}^{nucl}/MLL^{nucl}$ tumours. White arrows highlight cells co-expressing nuclear β-catenin and nuclear MLL. (**G**) Nuclear β-catenin correlates with nuclear MLL expression and both markers correlate with grade 3 human salivary gland SCC. β-Catenin and MLL expression was determined by immunofluorescence analysis in 13 SG-SCC. Associations were determined on an ordinal scale and evaluated using Kendall's Tau coefficient. *P*-values and patient numbers (n) are indicated. For details, see Supplementary Figure 7F and G; Supplementary Table 1 and Materials and methods. In (**C**–**E**), means and standard deviations are shown (*$P<0.05$, Student's *t*-test). *P*-values are as compared with control cells. Bar in (**C**, **F**); 25 μm. Source data for this figure is available on the online supplementary information page.

$CD24^+CD29^+$ cells into differentiation, whereas Ash1 siRNA had no effect (Figure 6E). siRNA treatments did not affect all cells, in contrast to ICG-001, possibly due to incomplete transfection efficacy (Figure 6C–E; Supplementary Figure 7D). In order to show that β-catenin and MLL are relevant in human salivary gland tumours, we evaluated the association of the gene products in the collection of 13 human SG-SCC specimens: nuclear β-catenin was associated with nuclear MLL, and both products significantly correlated with high-grade tumours (Figure 6F and G; Supplementary Figure 7F and G; $n=13$). This may also lead to an upregulation of other stem cell-associated genes, as exemplified for

NR5A2 (Supplementary Figure 7H). These data show that the association of nuclear β-catenin with nuclear MLL is of clinical relevance in human SG-SCC. Collectively, our data suggest that in both, murine and human tumours, the β-catenin/CBP/MLL axis drives self-renewal and fends off differentiation of tumour propagating cells via epigenetic mechanisms.

Discussion

Here, we report that mice with increased Wnt/β-catenin and attenuated Bmp signalling in Keratin 14-expressing tissues rapidly develop salivary gland SCC, from which we can enrich tumour propagating cells by FACS. The importance of canonical Wnt signalling in tumour propagating cells is known (Malanchi *et al*, 2008; Barker *et al*, 2009; Wend *et al*, 2010). We provide evidence that β-catenin activation leads to an induction and stabilization of MLL, and that β-catenin, CBP and MLL are required to trigger H3K4 tri-methylation at promoters of self-renewal genes in tumour propagating cells (summary scheme in Figure 7A).

Tumour propagating cells from salivary gland SCC of double mutants were enriched by FACS using high expression of the CD24 and CD29 surface antigens as markers, and 500 of sorted cells produced tumours upon serial transplantation in immune-compromised mice. Such serial transplantation experiments with low numbers of injected cells define tumour propagating cells, also called cancer stem cells (Prince *et al*, 2007; Gires, 2011; Nanduri *et al*, 2011; Visvader and Lindeman, 2012). The tumour propagating cells of salivary gland SCC retained the capacity to differentiate following transplantation, akin to cancer stem cells (Visvader and Lindeman, 2008). In our hands, other markers and marker combinations failed to isolate cells that could be used to generate tumours at this low number of injected cells. We also compared the tumour propagating cells from the double mutants with $CD24^+CD29^+$ cells of wild-type and single mutant salivary glands; this revealed that proliferation was significantly higher in double-mutant cells than in cells obtained from single mutants or control mice. Remarkably, 13% of the unsorted cells of tumours but 80–90% of the $CD24^+CD29^+$ cells were Ki67 positive in the double-mutant tissue. In conclusion, constitutive activation of Wnt/β-catenin signals strongly increase self-renewal of tumour propagating cells, while repression of BMP signals inhibits apoptosis, which in combination leads to permanently hyperproliferating salivary gland tumour cells.

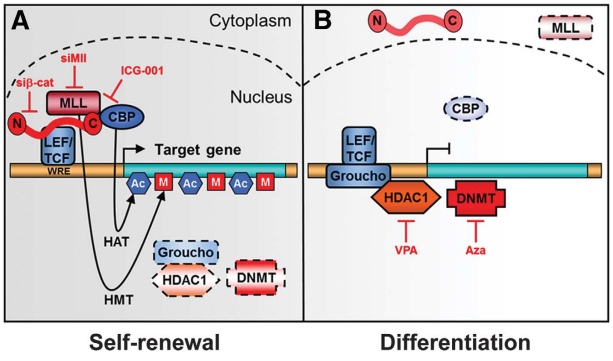

Figure 7 Model of self-renewal and differentiation of tumour propagating cells in salivary gland SCC. (**A**) Self-renewal depends on active Wnt/β-catenin signals, permissive chromatin, and expression of specific target genes, for example, pluripotency-associated genes. Potential histone methyltransferases (HMT; MLL) and histone acetyltransferases (HAT; CBP) bound to the C-terminus of β-catenin are shown. Genetic ablation of β-catenin or siRNAs against *Mll* inhibits interaction at Wnt-responsive elements (WRE). ICG-001 blocks association of CBP with β-catenin. (**B**) In contrast, differentiated tumour propagating cells exhibit inactive Wnt/β-catenin signalling, repressive chromatin, and downregulation of pluripotency-associated genes. Instead of β-catenin and associates, Groucho and DNMT may be bound to the WRE.

β-Catenin and CBP can tether MLL to promoters, where histone methyltransferase activity towards H3K4 is promoted (Taki *et al*, 1997; Emami *et al*, 2004; Dou *et al*, 2006; Mosimann *et al*, 2009; Arai *et al*, 2010). The trithorax-related MLL has been linked with gene activation and confers stem cell-like properties to haematopoietic cancer cells (Krivtsov and Armstrong, 2007; Visvader and Lindeman, 2008; Schuettengruber *et al*, 2011). Similarly, specific mutations of β-catenin bestow self-renewal properties to chronic myeloid leukaemia cells (Jamieson *et al*, 2004). MLL can exist in high molecular weight complexes with other methyltransferase components such as ASH2, which can enhance the activity of the MLL core complex (Southall *et al*, 2009). We found that high levels of nuclear β-catenin increase not only MLL, but also ASH2 levels in tumour propagating cells. Likewise, HELLS is upregulated in a Wnt/β-catenin-dependent manner in $CD24^+CD29^+$ tumour propagating cells. It is noteworthy that MLL expression depends on HELLS in prostate cancers (von Eyss *et al*, 2011). This suggests that the expression of a network of chromatin-associated proteins might be amplified by a feed-forward mechanism, ensuring that β-catenin–CBP–MLL has ample trithorax-related activity to maintain high H3K4me3 levels at target promoters. Further, differentiation of $CD24^+CD29^+$ tumour propagating cells is restored by downregulation of canonical Wnt signalling, that is, by ICG-001 or siRNA-mediated downregulation of β-catenin, CBP or MLL (scheme in Figure 7B). The temporal coordination of epigenetic reshaping and target gene expression in the differentiation of salivary gland tumour propagating cells supports the hypothesis that the tumour cells depend on Wnt/β-catenin–MLL-mediated epigenetic changes to suppress salivary gland differentiation. Finally, ICG-001-mediated differentiation of $CD24^+CD29^+$ tumour propagating cells cannot occur in the presence of the HDAC inhibitor VPA or the DNA methylation inhibitor 5-azacytidine, indicating that chromatin remodelling is also critical for differentiation (scheme in Figure 7B).

The strong effects of ICG-001 on tumour propagating cells might support new strategies for the development of rational therapies of solid tumours. Wnt/β-catenin signalling inhibitors eliminated stem cells in non-solid tumours, and ICG-001 eradicated drug-resistant leukaemic cancer stem cells *in vitro* and *in vivo* (Takahashi-Yanaga and Kahn, 2010). We show here that ICG-001 enforces differentiation of salivary gland tumour propagating cells in the mouse model, providing an efficient approach to target salivary gland cancer and potentially head and neck cancer in general. High Wnt/β-catenin and low Bmp signalling also correlate with the aggressiveness of human head and neck cancer and with the potential of the human tumour cells to self-renew. Moreover, the data with human cancers illustrate that nuclear β-catenin is significantly correlated with nuclear

MLL and high tumour grade. It will be important to test whether human head and neck cancers also respond to Wnt/β-catenin inhibitors.

Materials and methods

Mouse strains

K14Cre(Δneo), β-*catenin*^{floxEx3}, *Bmpr1a*^{flox} alleles and Cre-inducible lacZ reporter mice have been described, and mutant mice were analysed for genotype and recombination by PCR (Thorey *et al*, 1998; Harada *et al*, 1999; Huelsken *et al*, 2001; Mishina *et al*, 2002). The conditional gain-of-function mutation of β-catenin was produced by crossing homozygous mice carrying the β-*catenin*$^{lox(ex3)}$ allele to *K14-cre* mice. The loss-of-function mutation of *Bmpr1a* was produced by crossing homozygous mice carrying *Bmpr1a*^{flox} alleles to *K14-cre* mice that were homozygous for the *BmpRIA*^{flox} allele. To obtain the compound mutants, homozygous mice carrying the β-*catenin*$^{lox(ex3)}$ gain-of-function and the *BmpRIA*^{flox} loss-of-function allele were crossed with *K14-Cre* mice that were homozygous for the *Bmpr1a*^{flox} allele (a breeding scheme is shown in Supplementary Figure 1F). Animal experiments were performed according to the EU and national institutional regulations.

Immunodetection and other stainings

Immunohistochemistry, immunofluorescence and H&E staining were performed on frozen or formalin-fixed paraffin-embedded tissue sections as described (Huelsken *et al*, 2001). Human tumour samples were obtained from the Institute of Pathology, Charité-UKBF Berlin, Germany, and from the Department of Otorhinolaryngology, University Hospital Düsseldorf, Düsseldorf, Germany (for patient data, see Supplementary Table 1). Immunoblotting of westerns was performed using standard protocols: cells were lysed in HNTG buffer (20 mM HEPES pH 7.5, 150 mM NaCl, 1% (w/v) Triton X-10, 10% (w/v) glycerol). Histone extraction was performed according to the technical instructions from Abcam. Protein lysates were subjected to SDS–PAGE and transferred onto PVDF membranes. Membranes were incubated with specific antibodies, and western blots were developed using the chemiluminescence method (Perkin-Elmer). The following primary antibodies were used for immunodetection: mouse-anti-β-catenin (from BD Transduction Laboratories), rabbit-anti-phospho-Smad1/5/8, rabbit-anti-cleaved caspase-3, mouse-anti-CD44, rabbit-anti-Axin2, rabbit-anti-tri-methyl histone H3 (Lys4) (Cell Signaling), mouse-anti-CK10 and rabbit-anti-CK14 (Covance), Phycoerythrin (PE)-conjugated rat-anti-CD24 (BD Pharmingen), biotinylated goat-anti-CD29 (R&D Systems), rabbit-anti-phospho-histone H3 (Upstate), rabbit-anti-tri-methyl histone H3 (Lys9; Abcam), rabbit-anti-tri-methyl histone H3 (Lys27) (Millipore), rabbit-anti-MLL1 (Bethyl), rabbit-anti-Lamin (Santa Cruz) and mouse-anti-α-tubulin (Sigma).

Quantitative real-time PCR and microarray profiling

Isolation of total RNA, cDNA synthesis and qRT–PCR were performed using standard protocols: briefly, total RNA of tissue samples was isolated using Trizol (Invitrogen), and 5 μg total RNA was reverse transcribed using MMLV reverse transcriptase (Promega) according to the instructions by the manufacturers. qRT–PCR was performed using the iCycler IQTM 5 multicolor real-time detection system (Bio-Rad) with absolute SYBR green fluorescein (ABgene). PCR was carried out following a standard protocol: primer sequences used for qRT–PCR can be found in Supplementary Table 5. Microarray profiling was performed using GeneChip Mouse Genome 430 2.0 arrays (Affymetrix), following the protocol of the manufacturer. Profiling experiments are from salivary gland tissues of three mice in each group for the analysis at P1 and for the analysis of $CD24^+CD29^+$ stem cells at P90 (each $n=3$). Processing and statistical analysis of microarray data was performed using Genespring software.

Bioinformatics and GSEA of gene expression data and mouse survival statistics

Analysis of Affymetrix array data conformed to MIAME structure (http://www.mged.org). Log of ratio normalized expression data was analysed using a cross-gene error model and normalized according to the manufacturer protocol (GeneSpring software, Agilent). Assessment of differential expression was based on the highest achieved fold change and the lowest achieved *P*-value (Welch's *t*-test) and one-way-ANOVA with *P*-value cutoff of 0.05. No assumption of equality of variance was made, and Benjamini and Hochberg false discovery rates were used. A cutoff of 1.5-fold or greater expression difference was set to compare samples. GSEA was performed following the authors guidelines (Subramanian *et al*, 2005). We made use of gene sets representing biological pathways or gene ontology categories for biological processes, molecular functions and cellular compartments (http://www.broadinstitute.org/gsea/msigdb/). Each gene set was converted from human to mouse using the orthology mapping from The Jackson Laboratory (http://bioinf.wehi.edu.au/software/MSigDB). Kaplan–Meier survival curves of mice were calculated using SPSS 12.0 software (SPSS, Chicago), and differences in survival were assessed by the log-rank test. Survival analysis curves are representative of at least 21 mice for each genotype.

Cell preparation and FACS analysis

Salivary glands and primary tumour samples were collected, minced and incubated for 90 min at 37°C with digestion buffer containing DMEM/F12 1:1 (Invitrogen), 1.67 mg/ml collagenase (Invitrogen) and 1.33 mg/ml hyaluronidase (Sigma). The partly digested tissues were further treated for 60 min at 37°C with dispersion buffer containing DMEM/F12 (Invitrogen) and 1.67 mg/ml dispase (Invitrogen). Cell suspensions were passed through a stainless filter (70 μm) and centrifuged at 900 *g* for 5 min at 4°C. Pellets were suspended in 10 ml Dulbecco's modified Eagle/F12 1:1 medium and washed three times with PBS containing 10% fetal bovine serum (Invitrogen). After lysis of red blood cells in ice-cold 0.8% NH_4Cl (PBS), cells were washed three times with staining buffer (1% FBS/PBS) and incubated for 20 min with Fc receptor antibody (anti-mouse CD16/CD32; BD Pharmingen). Cells were washed three times with staining buffer and incubated with surface antigen antibodies for 45 min at 4°C. Primary antibodies were PE-conjugated rat-anti-CD24 (BD Pharmingen), biotinylated goat-anti-CD29 (R&D Systems), Allophycocyanin (APC)-conjugated CD29 (R&D Systems), mouse-anti-CD44 (Cell Signaling) and mouse-anti SSEA-1 antibody (R&D Systems). Samples were washed and incubated for 30 min at 4°C with secondary antibody, streptavidin-APC (Invitrogen) or Cy5 (BD Pharmingen). Cells were sorted using FACS Aria (BD Biosciences), and surface antigens of cells were analysed using a FACS caliber (BD Biosciences). Data were analysed using CELLQuest (BD Biosciences). Apoptotic cells were excluded by elimination of Dapi-positive cells. Gates were set to exclude 99.9% of cells labelled with isoform-matched control antibodies conjugated with the corresponding fluorochromes. Cytocentrifuge preparations were fixed in 4% formaldehyde and stained.

Xenograft experiments

$CD24^+CD29^+$-sorted and unsorted cells were transplanted at different dilutions subcutaneously into the back skin of NOD/SCID mice. Inhibition by ICG-001 in the NOD/SCID mouse xenograft model was investigated (each group $n=3$) as described (Emami *et al*, 2004).

Cell culture

Mouse cells were cultured in DMEM/F12 medium supplemented with 20% KSR (knockout serum replacement), non-essential minimal amino acids, penicillin/streptomycin, L-glutamine and β-mercaptoethanol (Invitrogen). Human head and neck carcinoma cell lines HNSCCUM-02T and HNSCCUM-03T were cultured as described (Welkoborsky *et al*, 2003). Cell proliferation was determined using the WST-1 cell proliferation assay (Roche) according to the instructions of the manufacturers. To test for non-adherent salisphere formation, cells were cultivated in a three-dimensional Matrigel (Invitrogen) layer for 24 h with culture medium and HGF at a concentration of 100 U/ml. Recombinant HGF was prepared as described (Brinkmann *et al*, 1995). After 24 h, cells were treated with ICG-001 (Emami *et al*, 2004), VPA (Enzo Life Sciences), 5-azacytidine (Sigma-Aldrich) or CHIR 99021 (Axon Medchem). For siRNA treatments, 30 pmol of various siRNAs (Dharmacon) was transfected by Lipofectamin (Invitrogen) according to the manufacturer's protocol. Cells were used for further experiments 48 h after transfection. All siRNA oligonucleotides were purchased from Dharmacon and used as pools of four specific oligos

(SMARTpool). RNAi oligonucleotide sequences are provided in Supplementary Table 6.

Time-course experiment

Salivary gland tumour propagating cells were plated at day 0. Starting from day 1, 25 μM of ICG-001 was added into culture medium at different time points allowing cells at different time points to be collected together and subjected to RT–PCR and western blot analysis. Cells at 0, 6, 12 and 24 h were incubated with equivalent concentration of compound vehicle (DMSO, 1%) before treated with ICG-001 to exclude the impact of vehicle on the cells.

Chromatin immunoprecipitation

In all, 10^6 cells were lysed and nuclear extracts prepared. These were incubated with 5 μg of antibody (rabbit-anti-tri-methyl histone H3 (Lys4; Cell Signaling) and 20 μl Protein A Sepharose beads (Invitrogen) in 500 μl PBS, 5 mg/ml BSA over night at 4°C. The beads were resuspended in 100 μl PBS and 5 mg BSA per ml chromatin, and the chromatin was incubated at 4°C on a rotating wheel. The beads were washed successively with 1 ml sonication buffer (50 mM Hepes pH 7.9, 140 mM NaCl, 1 mM EDTA, 1% Triton X-100, 0.1% Na-deoxycholate, 0.1% SDS, 0.25 mM PMSF and protease inhibitor cocktail (Roche), with 1 ml high salt buffer (same as sonication buffer except 500 mM NaCl) and with 1 ml LiCl wash buffer (20 mM Tris, pH 8.0, 1 mM EDTA, 250 mM LiCl, 0.5% NP-40, 0.5% Na-deoxycholate, 0.25 mM PMSF, protease inhibitor cocktail. All washing steps were repeated twice and performed on a rotating wheel at 4°C. The chromatin was eluted with 50 mM Tris, pH 8.0, 1 mM EDTA, 1% SDS, 50 mM $NaHCO_3$ at 65°C for 30 min. Primer sequences used for qRT–PCR of ChIP samples are provided in Supplementary Table 7.

Ultrastructural analysis of cells by electron microscopy

Cells were fixed with 4% formaldehyde, post-fixed with 1% OsO_4 for 45 min and contrasted with tannic acid and uranyl acetate. Specimens were dehydrated in a graduated ethanol series and embedded in PolyBed (Polysciences Europe GmbH). After polymerization, blocks were cut at 60–80 nm, contrasted with lead citrate and analysed in a LEO 906E TEM (Zeiss SMT) equipped with a Morada camera (SIS).

Supplementary data

Supplementary data are available at *The EMBO Journal* Online (http://www.embojournal.org).

Acknowledgements

We thank Dr C Birchmeier and R Hodge (MDC) for helpful discussion and critical reading of the manuscript, Dr H-P Rahn (MDC) for support with FACS and D Gerhard (MDC) for advice on animal experiments. We are indebted to RR Behringer for providing the $Bmpr1a^{lox}$ mice, to MM Taketo for the $\beta\text{-catenin}^{loxEx3}$ mice, and to RH Stauber for the HNSCCUM-02T and HNSCCUM-03T cell lines. PW was funded in part by the German Cancer Aid (Deutsche Krebshilfe). UZ was funded by a Marie Curie Excellence Grant.

Author contributions: PW and LF designed and performed experiments and analysed the data. QZ, FK, KE, VB and JDH performed experiments. JHS, CL and SH graded and screened human tumours. JHS, CL and MK provided material. JHS was involved in manuscript preparation. The biostatistics analysis for clinical relevance studies was conducted by SL. UZ and WB supervised the project, designed experiments and analysed the data. This manuscript was written by PW, UZ and WB. All authors reviewed the manuscript.

Conflict of interest

Dr Michael Kahn is a consultant, and equity holder in Prism Pharmaceuticals, which is developing the CBP/beta-catenin antagonist PRI-724.

References

Albert M, Peters AH (2009) Genetic and epigenetic control of early mouse development. *Curr Opin Genet Dev* **19:** 113–121

Arai M, Dyson HJ, Wright PE (2010) Leu628 of the KIX domain of CBP is a key residue for the interaction with the MLL transactivation domain. *FEBS Lett* **584:** 4500–4504

Barker N, Ridgway RA, van Es JH, van de Wetering M, Begthel H, van den Born M, Danenberg E, Clarke AR, Sansom OJ, Clevers H (2009) Crypt stem cells as the cells-of-origin of intestinal cancer. *Nature* **457:** 608–611

Barnes L, Eveson JW, Reichart P, Sidransky D (2005) *World Health Organization Classification of Tumours, Pathology & Genetics of Head and Neck Tumours*. Lyon: IARC Press

Behrens J, von Kries JP, Kuhl M, Bruhn L, Wedlich D, Grosschedl R, Birchmeier W (1996) Functional interaction of beta-catenin with the transcription factor LEF-1. *Nature* **382:** 638–642

Ben-Porath I, Thomson MW, Carey VJ, Ge R, Bell GW, Regev A, Weinberg RA (2008) An embryonic stem cell-like gene expression signature in poorly differentiated aggressive human tumors. *Nat Genet* **40:** 499–507

Brinkmann V, Foroutan H, Sachs M, Weidner KM, Birchmeier W (1995) Hepatocyte growth factor/scatter factor induces a variety of tissue-specific morphogenic programs in epithelial cells. *J Cell Biol* **131:** 1573–1586

Chu PG, Weiss LM (2002) Keratin expression in human tissues and neoplasms. *Histopathology* **40:** 403–439

Clay MR, Tabor M, Owen JH, Carey TE, Bradford CR, Wolf GT, Wicha MS, Prince ME (2010) Single-marker identification of head and neck squamous cell carcinoma cancer stem cells with aldehyde dehydrogenase. *Head Neck* **32:** 1195–1201

Clevers H (2006) Wnt/beta-catenin signaling in development and disease. *Cell* **127:** 469–480

De Napoles M, Mermoud JE, Wakao R, Tang YA, Endoh M, Appanah R, Nesterova TB, Silva J, Otte AP, Vidal M, Koseki H, Brockdorff N (2004) Polycomb group proteins Ring1A/B link ubiquitylation of histone H2A to heritable gene silencing and X inactivation. *Dev Cell* **7:** 663–676

Dou Y, Milne TA, Ruthenburg AJ, Lee S, Lee JW, Verdine GL, Allis CD, Roeder RG (2006) Regulation of MLL1 H3K4 methyltransferase activity by its core components. *Nat Struct Mol Biol* **13:** 713–719

Dou Y, Milne TA, Tackett AJ, Smith ER, Fukuda A, Wysocka J, Allis CD, Chait BT, Hess JL, Roeder RG (2005) Physical association and coordinate function of the H3 K4 methyltransferase MLL1 and the H4 K16 acetyltransferase MOF. *Cell* **121:** 873–885

Emami KH, Nguyen C, Ma H, Kim DH, Jeong KW, Eguchi M, Moon RT, Teo JL, Kim HY, Moon SH, Ha JR, Kahn M (2004) A small molecule inhibitor of beta-catenin/CREB-binding protein transcription [corrected]. *Proc Natl Acad Sci USA* **101:** 12682–12687

Fodde R, Brabletz T (2007) Wnt/beta-catenin signaling in cancer stemness and malignant behavior. *Curr Opin Cell Biol* **19:** 150–158

Gaspar-Maia A, Alajem A, Meshorer E, Ramalho-Santos M (2011) Open chromatin in pluripotency and reprogramming. *Nat Rev Mol Cell Biol* **12:** 36–47

Gires O (2011) Lessons from common markers of tumor-initiating cells in solid cancers. *Cell Mol Life Sci* **68:** 4009–4022

Goldberg AD, Allis CD, Bernstein E (2007) Epigenetics: a landscape takes shape. *Cell* **128:** 635–638

Grigoryan T, Wend P, Klaus A, Birchmeier W (2008) Deciphering the function of canonical Wnt signals in development and disease: conditional loss- and gain-of-function mutations of beta-catenin in mice. *Genes Dev* **22:** 2308–2341

Hai B, Yang Z, Millar SE, Choi YS, Taketo MM, Nagy A, Liu F (2010) Wnt/beta-catenin signaling regulates postnatal development and regeneration of the salivary gland. *Stem Cells Dev* **19:** 1793–1801

Harada N, Tamai Y, Ishikawa T, Sauer B, Takaku K, Oshima M, Taketo MM (1999) Intestinal polyposis in mice with a dominant stable mutation of the beta-catenin gene. *EMBO J* **18:** 5931–5942

Heng JC, Feng B, Han J, Jiang J, Kraus P, Ng JH, Orlov YL, Huss M, Yang L, Lufkin T, Lim B, Ng HH (2010) The nuclear receptor Nr5a2 can replace Oct4 in the reprogramming of murine somatic cells to pluripotent cells. *Cell Stem Cell* **6:** 167–174

Hisatomi Y, Okumura K, Nakamura K, Matsumoto S, Satoh A, Nagano K, Yamamoto T, Endo F (2004) Flow cytometric isolation of endodermal progenitors from mouse salivary gland differentiate into hepatic and pancreatic lineages. *Hepatology (Baltimore, MD)* **39:** 667–675

Huelsken J, Vogel R, Erdmann B, Cotsarelis G, Birchmeier W (2001) Beta-catenin controls hair follicle morphogenesis and stem cell differentiation in the skin. *Cell* **105:** 533–545

Jamieson CH, Ailles LE, Dylla SJ, Muijtjens M, Jones C, Zehnder JL, Gotlib J, Li K, Manz MG, Keating A, Sawyers CL, Weissman IL (2004) Granulocyte-macrophage progenitors as candidate leukemic stem cells in blast-crisis CML. *N Engl J Med* **351:** 657–667

Kim SK, Suh MR, Yoon HS, Lee JB, Oh SK, Moon SY, Moon SH, Lee JY, Hwang JH, Cho WJ, Kim KS (2005) Identification of developmental pluripotency associated 5 expression in human pluripotent stem cells. *Stem Cells (Dayton, Ohio)* **23:** 458–462

Krivtsov AV, Armstrong SA (2007) MLL translocations, histone modifications and leukaemia stem-cell development. *Nat Rev Cancer* **7:** 823–833

Lombaert IM, Brunsting JF, Wierenga PK, Faber H, Stokman MA, Kok T, Visser WH, Kampinga HH, de Haan G, Coppes RP (2008) Rescue of salivary gland function after stem cell transplantation in irradiated glands. *PLoS ONE* **3:** e2063

Lustig B, Jerchow B, Sachs M, Weiler S, Pietsch T, Karsten U, van de WM, Clevers H, Schlag PM, Birchmeier W, Behrens J (2002) Negative feedback loop of Wnt signaling through upregulation of conductin/axin2 in colorectal and liver tumors. *Mol Cell Biol* **22:** 1184–1193

Malanchi I, Peinado H, Kassen D, Hussenet T, Metzger D, Chambon P, Huber M, Hohl D, Cano A, Birchmeier W, Huelsken J (2008) Cutaneous cancer stem cell maintenance is dependent on beta-catenin signalling. *Nature* **452:** 650–653

Man YG, Ball WD, Marchetti L, Hand AR (2001) Contributions of intercalated duct cells to the normal parenchyma of submandibular glands of adult rats. *Anat Rec* **263:** 202–214

Mishina Y, Hanks MC, Miura S, Tallquist MD, Behringer RR (2002) Generation of Bmpr/Alk3 conditional knockout mice. *Genesis* **32:** 69–72

Molenaar M, van de Wetering M, Oosterwegel M, Peterson-Maduro J, Godsave S, Korinek V, Roose J, Destree O, Clevers H (1996) XTcf-3 transcription factor mediates beta-catenin-induced axis formation in Xenopus embryos. *Cell* **86:** 391–399

Monroe MM, Anderson EC, Clayburgh DR, Wong MH (2011) Cancer stem cells in head and neck squamous cell carcinoma. *J Oncol* **2011:** 762780

Mosimann C, Hausmann G, Basler K (2009) Beta-catenin hits chromatin: regulation of Wnt target gene activation. *Nat Rev Mol Cell Biol* **10:** 276–286

Nanduri LS, Maimets M, Pringle SA, van der Zwaag M, van Os RP, Coppes RP (2011) Regeneration of irradiated salivary glands with stem cell marker expressing cells. *Radiother Oncol* **99:** 367–372

Parker DS, Ni YY, Chang JL, Li J, Cadigan KM (2008) Wingless signaling induces widespread chromatin remodeling of target loci. *Mol Cell Biol* **28:** 1815–1828

Piccirillo SG, Reynolds BA, Zanetti N, Lamorte G, Binda E, Broggi G, Brem H, Olivi A, Dimeco F, Vescovi AL (2006) Bone morphogenetic proteins inhibit the tumorigenic potential of human brain tumour-initiating cells. *Nature* **444:** 761–765

Prince ME, Sivanandan R, Kaczorowski A, Wolf GT, Kaplan MJ, Dalerba P, Weissman IL, Clarke MF, Ailles LE (2007) Identification of a subpopulation of cells with cancer stem cell properties in head and neck squamous cell carcinoma. *Proc Natl Acad Sci USA* **104:** 973–978

Read TA, Fogarty MP, Markant SL, McLendon RE, Wei Z, Ellison DW, Febbo PG, Wechsler-Reya RJ (2009) Identification of CD15 as a marker for tumor-propagating cells in a mouse model of medulloblastoma. *Cancer Cell* **15:** 135–147

Ring DB, Johnson KW, Henriksen EJ, Nuss JM, Goff D, Kinnick TR, Ma ST, Reeder JW, Samuels I, Slabiak T, Wagman AS, Hammond ME, Harrison SD (2003) Selective glycogen synthase kinase 3 inhibitors potentiate insulin activation of glucose transport and utilization in vitro and in vivo. *Diabetes* **52:** 588–595

Schuettengruber B, Martinez AM, Iovino N, Cavalli G (2011) Trithorax group proteins: switching genes on and keeping them active. *Nat Rev Mol Cell Biol* **12:** 799–814

Sierra J, Yoshida T, Joazeiro CA, Jones KA (2006) The APC tumor suppressor counteracts beta-catenin activation and H3K4 methylation at Wnt target genes. *Genes Dev* **20:** 586–600

Sneddon JB, Werb Z (2007) Location, location, location: the cancer stem cell niche. *Cell Stem Cell* **1:** 607–611

Southall SM, Wong PS, Odho Z, Roe SM, Wilson JR (2009) Structural basis for the requirement of additional factors for MLL1 SET domain activity and recognition of epigenetic marks. *Mol Cell* **33:** 181–191

Speight PM, Barrett AW (2002) Salivary gland tumours. *Oral Dis* **8:** 229–240

Stewart BW, Kleihues P (2003) *World Cancer Report*. Lyon: World Health Organization, IARC

Subramanian A, Tamayo P, Mootha VK, Mukherjee S, Ebert BL, Gillette MA, Paulovich A, Pomeroy SL, Golub TR, Lander ES, Mesirov JP (2005) Gene set enrichment analysis: a knowledge-based approach for interpreting genome-wide expression profiles. *Proc Natl Acad Sci USA* **102:** 15545–15550

Surani MA, Hayashi K, Hajkova P (2007) Genetic and epigenetic regulators of pluripotency. *Cell* **128:** 747–762

Takahashi-Yanaga F, Kahn M (2010) Targeting Wnt signaling: can we safely eradicate cancer stem cells? *Clin Cancer Res* **16:** 3153–3162

Taki T, Sako M, Tsuchida M, Hayashi Y (1997) The t(11;16)(q23;p13) translocation in myelodysplastic syndrome fuses the MLL gene to the CBP gene. *Blood* **89:** 3945–3950

Thorey IS, Muth K, Russ AP, Otte J, Reffelmann A, von Melchner H (1998) Selective disruption of genes transiently induced in differentiating mouse embryonic stem cells by using gene trap mutagenesis and site-specific recombination. *Mol Cell Biol* **18:** 3081–3088

Tucker AS (2007) Salivary gland development. *Semin Cell Dev Biol* **18:** 237–244

Visvader JE, Lindeman GJ (2008) Cancer stem cells in solid tumours: accumulating evidence and unresolved questions. *Nat Rev* **8:** 755–768

Visvader JE, Lindeman GJ (2012) Cancer stem cells: current status and evolving complexities. *Cell Stem Cell* **10:** 717–728

von Eyss B, Maaskola J, Memczak S, Mollmann K, Schuetz A, Loddenkemper C, Tanh MD, Otto A, Muegge K, Heinemann U, Rajewsky N, Ziebold U (2011) The SNF2-like helicase HELLS mediates E2F3-dependent transcription and cellular transformation. *EMBO J* **31:** 972–985

Ware CB, Wang L, Mecham BH, Shen L, Nelson AM, Bar M, Lamba DA, Dauphin DS, Buckingham B, Askari B, Lim R, Tewari M, Gartler SM, Issa JP, Pavlidis P, Duan Z, Blau CA (2009) Histone deacetylase inhibition elicits an evolutionarily conserved self-renewal program in embryonic stem cells. *Cell Stem Cell* **4:** 359–369

Welkoborsky HJ, Jacob R, Riazimand SH, Bernauer HS, Mann WJ (2003) Molecular biologic characteristics of seven new cell lines of squamous cell carcinomas of the head and neck and comparison to fresh tumor tissue. *Oncology* **65:** 60–71

Wend P, Holland JD, Ziebold U, Birchmeier W (2010) Wnt signaling in stem and cancer stem cells. *Semin Cell Dev Biol* **21:** 855–863

Wend P, Runke S, Wend K, Anchondo B, Yesayan M, Jardon M, Hardie N, Loddenkemper C, Ulasov I, Lesniak MS, Wolsky R, Bentolila LA, Grant SG, Elashoff D, Lehr S, Latimer JJ, Bose S, Sattar H, Krum SA, Miranda-Carboni GA (2013) WNT10B/beta-catenin signalling induces HMGA2 and proliferation in metastatic triple-negative breast cancer. *EMBO Mol Med* **5:** 264–279

Whitman M (1998) Smads and early developmental signaling by the TGFbeta superfamily. *Genes Dev* **12:** 2445–2462

Xi S, Geiman TM, Briones V, Guang Tao Y, Xu H, Muegge K (2009) Lsh participates in DNA methylation and silencing of stem cell genes. *Stem cells (Dayton, Ohio)* **27:** 2691–2702

Ying YL, Johnson JT, Myers EN (2006) Squamous cell carcinoma of the parotid gland. *Head Neck* **28:** 626–632